ELSEVIER

Carbohydrate Research 315 (1999) 48–62

CARBOHYDRATE RESEARCH

NMR study of a Lewis^X pentasaccharide derivative: solution structure and interaction with cations

Benoît Henry [a], Hervé Desvaux [a], Marina Pristchepa [a], Patrick Berthault [a,*], Yong-Min Zhang [b], Jean-Maurice Mallet [b], Jacques Esnault [b], Pierre Sinaÿ [b]

[a] *CEA Saclay, Laboratoire Commun de RMN, DSM/DRECAM/SCM, F-91191 Gif sur Yvette, France*
[b] *Ecole Normale Supérieure, Département de Chimie, Associé au CNRS, 24 rue Lhomond, F-75231 Paris, France*

Received 7 October 1998; accepted 19 November 1998

Abstract

The structure and conformation of the synthetic pentasaccharide Gal(β1-4){Fuc(α1-3)}GlcNAc(β1-3)Gal(β1-4)Glc-βOMe of the Lewis^X family has been determined by NMR spectroscopy in dimethyl sulfoxide and methanol. In these solvents, the binding constants with calcium have been evaluated as 9.5 and 29.6 M^{-1}, respectively. Study of the interaction sites has been achieved through the use of paramagnetic divalent cations and distance triangulation methods. Two regions have been found, the first one in the vicinity of the fucose unit, the second one closer to the lactose part.

Keywords: Lewis^X; Oligosaccharide; Paramagnetic ions; Calcium; ^{1}H NMR; ^{13}C NMR

1. Introduction

The molecular basis of cell recognition and adhesion is of paramount importance for understanding biological phenomena such as differentiation, organisation and development in multicellular organisms, as well as diseases involving abnormal cell adhesion. It has been demonstrated that specific interaction between carbohydrates may be an important initial step in such cellular processes [1–3].

Specific interaction between Le^x and Le^x determinants of glycosphingolipids has been studied by Hakomori et al. [4,5]. It may provide an interesting possible basis for cell recognition in preimplantation embryos and in embryonal carcinoma cells. Such a homotypic interaction between two neutral oligosaccharides is mediated by the presence of Ca^{2+}, Mg^{2+}, or Mn^{2+}. The association of neutral carbohydrates and polyols with metal cations in solution has been studied [6–8], using a wide range of analytical techniques: electrophoresis [9,10], thin-layer chromatography [11], Fourier-transform infrared spectroscopy [12], microcalorimetry [13], ebulliometry [6], luminescence excitation spectroscopy [14], pHmetry [15], etc., but it is only when nuclear magnetic resonance spectroscopy [16] or mass spectrometry [17–19] has been used that more precise information about the structure of the complex could be obtained.

Although high-resolution liquid-state NMR spectroscopy is a very powerful tool for elucidation of intermolecular events, evidencing carbohydrate–carbohydrate interaction such as Le^x–Le^x with the help of this spectroscopy

* Corresponding author. Tel.: +33-1-69084245; fax: +33-1-69089806.
E-mail address: patrick.berthault@cea.fr (P. Berthault)

0008-6215/99/$ - see front matter
PII: S0008-6215(98)00301-2

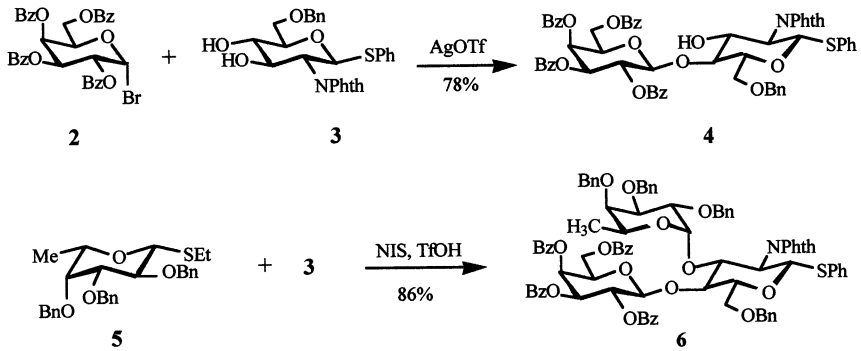

Scheme 1.

remains difficult. Indeed this phenomenon takes profit in situ from a cooperative effect, made possible by the high density of sugar headgroups at the cell surface. Some attempts to mimic this glycoside-enriched surface for NMR studies have made use of ganglioside micelles. However, even in such conditions, it has not been possible to evidence carbohydrate–carbohydrate interactions [20].

It appears to us that a knowledge of the structure, internal dynamics in solution, and interaction with divalent cations of Le^X derivatives through NMR is a prerequisite to the study of site-specific homotypic interaction. Wormald et al. have failed in showing specific or general interaction of Le^X and the pentasaccharide (Gal(β1-4){Fuc(α1-3)}GlcNAc(β1-3)Gal(β1-4)Glc) oligosaccharides with Ca^{2+} or Mn^{2+} [21]. Their study used ^1H NMR in D_2O, and no detectable change in the proton chemical shifts of the sugars was observed. As hydroxyl groups represent the external surface of an oligosaccharide, the signals of their protons are expected to experience more significant effects upon weak interaction with an ion than the non-labile ones. For this reason, we have undertaken an NMR study of a pentasaccharide containing the Le^X motif, in dimethyl sulfoxide and in methanol, where these signals can easily be observed. Moreover, the binding constants with calcium are expected to be greater in methanol than in water [22].

The molecular structure of this pentasaccharide **1** is very close to the Wormald et al. pentasaccharide, except that the terminal glucose unit retains the β-configuration as methyl glycoside.

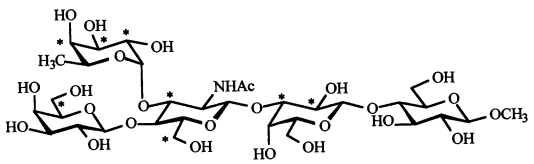

1

*Asterisks indicate protons which show the largest chemical shift variation upon addition of Ca^{2+} ions

The first experiments deal with the precise analysis of the structure and internal dynamics of this oligosaccharide in solution through recent dedicated approaches [23–25]. Influence of Ca^{2+} ions on the proton spectra is then studied in order to derive the corresponding association constants. A third type of experiment uses paramagnetic ions to mimic complexation of calcium ions as detected by ^1H and ^{13}C NMR, and to allow the determination of their location relative to structure **1**.

2. Experimental

Synthesis of pentasaccharide **1**.—Compound **1** was prepared efficiently as follows: reaction in CH_2Cl_2 of bromide **2** [26] (Scheme 1) with the known diol **3** [27], using silver trifluoromethanesulfonate (AgOTf) as the promoter, gave the disaccharide **4**.

The regiochemistry of the newly introduced glycosidic linkage was confirmed by the ^1H NMR data which show a signal for Glc H-3 at 4.64 ppm (ddd, $J_{3,OH}$ 1.2 Hz, $J_{3,4}$ 8.6 Hz, $J_{2,3}$ 10.4 Hz). Its stereochemistry was determined to be β on the basis of the Gal H-1–H-2 coupling constant ($J_{1,2}$ 8.1 Hz). The fucosylation of **4** with ethyl 2,3,4-tri-*O*-benzyl-1-thio-β-L-fucopyranoside **5** [28] in the presence of

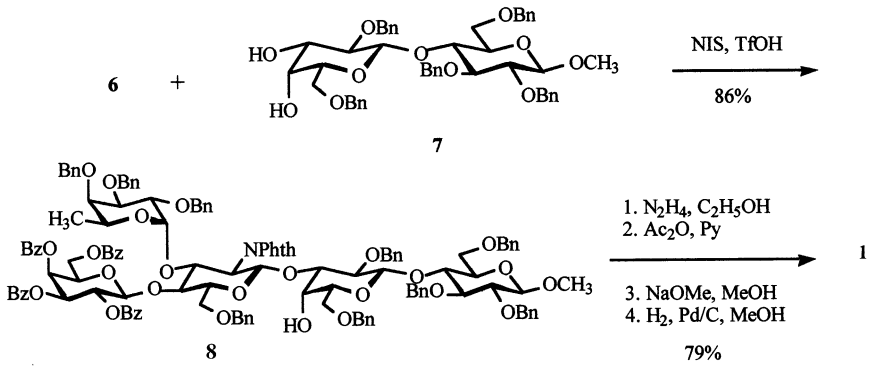

Scheme 2.

N-iodosuccinimide (NIS)–trifluoromethanesulfonic acid (TfOH) [29] provided the trisaccharide **6** in 86% yield. It was therefore possible to activate the armed SEt group without affecting the disarmed SPh group by using 1 equiv of NIS [30]. The stereochemistry of the newly introduced glycosidic linkage was determined to be α on the basis of the low value of the Fuc H-1–H-2 coupling constant ($J_{1,2}$ 3.5 Hz).

The coupling of **6** and methyl 2,3,6-tri-*O*-benzyl-4-*O*-(2,6-di-*O*-benzyl-β-D-galactopyranosyl)-β-D-glucopyranoside **7**, easily prepared from methyl β-D-lactoside [31], was performed in the conditions described above, generating the pentasaccharide **8** in 86% yield (Scheme 2).

The stereochemistry of the newly introduced linkage was determined to be β on the basis of the GlcN H-1–H-2 coupling constant ($J_{1,2}$ 8.5 Hz). The regioselectivity of the glycosylation was confirmed by acetylation of **8**. The ^{1}H NMR spectrum of the acetate showed the presence of H-4 of the galactose unit at 5.42 ppm (dd, $J_{4,5} < 1$ Hz, $J_{3,4} = 3.5$ Hz), indicating the position of the new glycosidic linkage in **8** to be at OH-3 of the acceptor **7**. Classical deprotections gave the expected pentasaccharide **1**. A detailed experimental part will be published elsewhere.

NMR spectroscopy.—Before each NMR experiment, the samples were freeze-dried and accurately weighed in the NMR tube. They were then dissolved either in $(CD_3)_2SO$, in CD_3OH, or in CD_3OD (all originating from CEA, Eurisotop). All experiments were performed on Bruker DRX spectrometers equipped with self-shielded gradient ^{1}H/^{13}C/^{15}N 5-mm inverse probeheads, at 11.7 and 14 Tesla. Assignment of the proton chemical shifts of **1** was performed through homonuclear and heteronuclear 1D and 2D NMR experiments in CD_3OH and CD_3OD. The main ^{1}H NMR experiments were COSY, RELAYs and TOCSY for determination of the intra-unit through-bond connectivities, and off-resonance ROESY for the inter-unit sequencing. Carbon assignment was achieved by inverse HMQC [32,33] and HMBC [34] experiments.

The conformation and the internal dynamics of the oligosaccharide in methanol were determined by the use of a proton NMR method that was recently proposed by us [25]. It has the advantage of avoiding the requirement of an internal distance reference to derive the other interproton distances. For this purpose, 27 2D off-resonance ROESY experiments with effective spin-lock flip angles ranging from 0 to 54.7° and mixing times between 50 and 150 ms were performed, as well as numerous 1D off-resonance ROESY to complete them when a high resolution was needed. After assumption of a simple motional model, where the dipolar auto-correlation function associated to each proton pair can be described by an exponential function, 66 H–H distance constraints and 66 local correlation times were derived for the pentasaccharide in the absence of calcium. For pentasaccharide **1** in the presence of calcium, as most of the hydroxyl proton signals were broadened by exchange with the solvent, they do not give rise to dipole–dipole cross-peaks with the neighbouring protons. Therefore only 49 distance constraints are derived in this case.

Molecular modelling.—The H–H distance constraints obtained after off-resonance ROESY are used in a simulated annealing procedure using X-PLOR 3.1 software facilities [35]. Starting 50 times from a different random conformation, 50 structures were generated after 35 ps of high temperature (1000 K) dynamics and slow cooling during 28 ps, both with a timestep of 3.5 fs. During the high-temperature dynamics, progressive introduction of the distance constraints with low weight on the van der Waals terms ensured a large sampling of the conformational space. The slow cooling was designed to restore the correct values of the covalent energy terms. According to criteria based on the NMR constraints and covalent energy terms, some resulting structures were rejected, and the remaining set was used to compute the average structure and the rms deviations on the coordinates.

Calcium titration.—In $(CD_3)_2SO$, the starting solution was constituted of **1** (3.51 mg) in 400 μL at 295 K (concentration: 10.1 mM). From 0 to 37.9 equiv of $CaCl_2{\cdot}2H_2O$ were added at two concentrations: 808 mM and 80.8 mM. In CD_3OD, the starting solution was constituted of **1** (3.91 mg) in 360 μL at 290 K (concentration: 12.5 mM). From 0 to 7.55 equiv of $CaCl_2{\cdot}2H_2O$ were added from a solution of 120 mM.

Correcting the dilution and pH variation effects, the observed chemical shift variation of a given signal upon addition of an ion in solution can be expressed as:

$$\Delta\delta_{obs} = \Delta\delta_{struc} + \Delta\delta_{dia} + \Delta\delta_{pseudo\text{-}contact} + \Delta\delta_{contact} \quad (1)$$

where $\Delta\delta_{struc}$ represents the chemical shift variation due to conformational modification of the molecule upon addition of the ion, $\Delta\delta_{dia}$ the diamagnetic susceptibility shift, and $\Delta\delta_{pseudo\text{-}contact}$, $\Delta\delta_{contact}$ the paramagnetic pseudo-contact and contact hyperfine coupling terms, respectively. In the case of calcium, the last two terms vanish. As fast exchange conditions are fulfilled and assuming a 1:1 complex, $\Delta\delta_{obs}$ can also be expressed as, after correction of the global susceptibility shift of the sample:

$$\Delta\delta_{obs} = \delta_{obs} - \delta_{free} = (\delta_{complex} - \delta_{free})\ K[Ca]\ (1 + K[Ca])^{-1} \quad (2)$$

An iterative program based on the Marquardt algorithm [36] allows the determination of the association constant K as well as $\delta_{complex}$, the chemical shift of each proton in the pure complex. The fit used simultaneously every peak exhibiting a chemical shift variation. In this way a large oversampling of the system was secured.

Use of paramagnetic ions in NMR.—To avoid any inner-sphere complexation with the cations studied, chloride was chosen as a counter-ion for every experiment [37,38].

Mn^{2+}. Four ^{13}C longitudinal self-relaxation experiments were performed with equivalents of $MnCl_2$ ranging from 0 to 0.025 (0, 0.005, 0.015, 0.025). The initial concentration of **1** in methanol was 57 mM. The dilution effect upon addition of $MnCl_2{\cdot}2H_2O$ was negligible.

Co^{2+}. A 2D COSY experiment was used to univocally assign the maximum of proton signals in the presence of 0.5 equiv of $CoCl_2$. Due to line broadening at higher concentrations, we were not able to determine the equilibrium constant with the cation, and only one addition of cobalt was used for determining the interaction sites. The concentration of **1** in methanol was 9.2 mM. The dilution effect upon addition of $CoCl_2{\cdot}2H_2O$ was negligible.

Location of Mn^{2+} and Co^{2+}.—On each of the accepted structures after simulated annealing, the Cartesian coordinates of two Mn^{2+} ions were randomly drawn in order to ensure coverage of the subspace of solutions as complete as possible, and to allow a statistical analysis. The most probable location of the ions was determined through a simplex procedure [36] which minimised the following target function, using the relative variations of the ^{13}C self-relaxation rates $\Delta(1/T_1^i)$ due to addition of Mn^{2+}:

$$\chi^2 = \sum_i \frac{1}{\sigma_i^2} \left(\frac{\Delta\left(\frac{1}{T_1^i}\right)}{\Delta\left(\frac{1}{T_1^{ref}}\right)} - \frac{r_{I^i}^{-6} + r_{II^i}^{-6}}{r_{I^{ref}}^{-6} + r_{II^{ref}}^{-6}} \right)^2 \quad (3)$$

The summation was done on all the carbons for which the longitudinal self-relaxation rates had been measured (all except those exhibiting overlapped signals). The back calculated distance between the Mn^{2+} ion and the ith carbon (subscripts I and II refer to the manganese ion considered) is denoted as r^i. The reference (subscript ref) was taken as the carbon for which the largest variation on $(1/T_1)$ was observed (i.e. Gal^I C-6). σ_i was the estimated uncertainty. The consideration of different populations for the two locations of the cation does not induce a significant improvement of the minimised χ^2 value. The resulting coordinates inside a cube $40 \times 40 \times 40$ Å^3 centred on the molecular coordinates, and with a low χ^2 value, were kept and clustered in pieces of $0.2 \times 0.2 \times 0.2$ Å^3. Then the average locations of the two ions were computed, as well as the rmsd along the coordinates.

For cobalt, the same principle as for manganese was used. But instead of six variables which correspond to the six coordinates (x_I, y_I, z_I, x_{II}, y_{II}, z_{II}), there were ten variables to consider (the same, plus θ_I, ϕ_I, θ_{II}, ϕ_{II}, which define the principal axes of the paramagnetic susceptibility tensors for the cobalt ions in the pentasaccharide molecular frame). The function to be minimised, which takes into account the ratio of the paramagnetic dipolar shifts, is:

$$\chi^2 = \sum_i \frac{1}{\sigma_i^2} \left(\frac{\Delta\delta_i}{\Delta\delta_{ref}} - \frac{\dfrac{3\cos^2 \Psi_{Ii} - 1}{r_{Ii}^3} + \dfrac{3\cos^2 \Psi_{IIi} - 1}{r_{IIi}^3}}{\dfrac{3\cos^2 \Psi_{Iref} - 1}{r_{Iref}^3} + \dfrac{3\cos^2 \Psi_{IIref} - 1}{r_{IIref}^3}} \right)^2 \quad (4)$$

$\Delta\delta_i$, $\Delta\delta_{ref}$ are the chemical shift variations of protons i and reference, respectively. The angle between the principal axis of the Co^{2+} anisotropic susceptibility tensor and the vector r_i joining the Co^{2+} ion and the considered nucleus is denoted Ψ. Similarly to what was done for manganese, and in order to minimise the relative error, the proton chosen as reference was the one for which the largest chemical shift variation was observed (Gal^I H-6). In this operation, assumptions were made that the contact term was negligible, and secondly that the cobalt ion was of axial symmetry [39]. Due to the too high number of parameters to adjust in a direct fit, it was difficult to be sure that the random drawing of the parameters was sufficiently wide to explore the complete subspace of solutions, and then to perform confident statistical tests. We consequently used the following procedure. The results on the best-fit manganese coordinates were used as starting points for the Co^{2+} ions, and only θ_I, ϕ_I, θ_{II}, ϕ_{II} were refined in a first step. Then noise was added to the ten parameters (the best-fit coordinates found for Mn^{2+} and these four angles), and this full set was again refined by the same simplex procedure against Eq. (4). As well as for Mn^{2+}, the introduction of a difference in population between the two cobalt locations, which would mean a different binding constant or paramagnetic contribution, does not increase significantly the χ^2, because of the poor ratio between the number of experimental data and the number of parameters to be minimised (42 vs. 10). The solutions for the cobalt locations were then treated by the same procedure as for manganese.

Obviously, the location of the ion was strongly dependent of the pentasaccharide 3D structure. For describing the results, two types of distance average were measured. Either for each **1** structure, the average location of the ion, denoted $\langle X \rangle$, was considered to evaluate some representative distances with atoms of the pentasaccharide. Or each location of the ion obtained after the minimisation step was used to calculate the distances with atoms of the pentasaccharide; then the complete ensemble average was computed on all the locations and all the structures possible for **1**. These two methods lead to results that are similar but not identical, since the distributions are not Gaussian.

3. Results and discussion

Solution structure of pentasaccharide **1**.— The preliminary step before determination of the 3D structure by NMR is the assignment

Table 1
^{13}C and ^{1}H chemical shifts for **1** in $(CD_3)_2SO$ at 290 K using $(CD_3)_2SO$ as internal reference (^{13}C, 39.5 ppm; ^{1}H, 2.50 ppm)[a]

	C-1	C-2	C-3	C-4	C-5	C-6		CH_3
Gal^{I}	101.93	70.45	73.21	67.08	74.39	59.55		
Fuc^{II}	98.34	64.08	69.17	71.40	46.54			16.18
$GlcNAc^{III}$	101.15	55.46	75.14	73.32	75.43	59.27		22.84
Gal^{IV}	103.26	69.07	82.09	66.86	74.81	60.06		
Glc^{V}	103.35	72.86	74.55	74.55	80.27	60.11		55.89
	H-1	H-2	H-3	H-4	H-5	H-6	H-6′	CH_3
Gal^{I}	4.268	3.272	3.221	3.643	3.218	3.520	3.397	
Fuc^{II}	4.824	3.391	3.540	3.450	4.650			0.985
$GlcNAc^{III}$	4.688	3.613	3.689	3.621	3.308	3.791	3.660	1.805
Gal^{IV}	4.252	3.423	3.421	3.861	3.480	3.524	3.480	
Glc^{V}	4.096	2.997	3.297	3.300	3.296	3.753	3.605	3.390
	HO-1	HO-2	HO-3	HO-4	HO-5	HO-6		
Gal^{I}		5.010	4.737	4.240		4.485		
Fuc^{II}		3.082	4.247	4.107				
$GlcNAc^{III}$						4.701		
Gal^{IV}		4.919		4.688		4.721		
Glc^{V}		5.207	4.616			4.615		

[a] The notations H-6, H-6′ do not refer to pro-*R* and pro-*S* protons, as no stereospecific assignment has been done.

of the proton and carbon chemical shifts. Although this has been achieved both in dimethyl sulfoxide and in methanol, in the following development, for the conformational analysis of the oligosaccharide, emphasis has been put on the analysis in methanol.

Comparison of the proton chemical shifts of **1** in $(CD_3)_2SO$ and in CD_3OD (Tables 1 and 2) shows no big difference between them, which could indicate that the structure is not strongly modified between the two solvents.

As the common problem encountered in the resolution of molecular structures through high-resolution NMR is how to differentiate a high flexibility from a lack of NMR data for a part of the molecule, we preferred to avoid a direct comparison between the 3D structure of **1** in the presence and in the absence of calcium in CD_3OH. Indeed as the exchange rates with solvent are rather different in both cases (see below), it could lead to the erroneous interpretation that the structure in the absence of calcium is more rigid than the other one, even if we have potent NMR methods to get information on the local dynamics.

A second argument for avoiding such a comparison is that the accuracy on the interproton distance information is not high enough to draw conclusions on slight variations of the orientation of a unit relative to another one. This comparison could be made only if a drastic conformation change occurred after addition of calcium, effect which does not appear. Therefore, the following part of the text only presents the molecular modelling results for the study of the pentasaccharide alone or in the presence of 11.4 equiv of calcium in CD_3OD; only some indicative comparisons are given.

For the study of the pentasaccharide alone in methanol, after the simulated annealing procedure, only 27 structures were kept. The remaining ones were rejected, because their potential energy was too high. The rms deviation for the coordinates of the heavy atoms of the accepted structures was 1.02 Å.

For the study of the pentasaccharide **1** in methanol in the presence of calcium, 35 structures were kept according to the same

Table 2
^{13}C and ^{1}H chemical shifts for **1** in CD_3OD at 290 K[a]

	C-1	C-2	C-3	C-4	C-5	C-6		CH_3
1								
Gal^{I}	103.79	72.64	74.74	69.90	76.80	62.70		
Fuc^{II}	100.25	69.82	71.09	73.64	67.53			16.68
$GlcNAc^{III}$	103.76	57.73	71.05	76.27	76.49	61.02		23.19
Gal^{IV}	104.85	71.51	83.80	69.79	78.48	62.55		
Glc^{V}	105.18	74.57	76.25	80.28	76.44	61.56		57.29
	H-1	H-2	H-3	H-4	H-5	H-6	H-6′	CH_3
1								
Gal^{I}	4.478	3.550	3.500	3.839	3.491	3.712	3.806	
Fuc^{II}	5.098	3.683	3.912	3.764	4.890			1.219
$GlcNAc^{III}$	4.733	3.975	3.903	3.951	3.468	3.921	4.010	2.025
Gal^{IV}	4.408	3.645	3.596	4.101	3.635	3.726	3.823	
Glc^{V}	4.244	3.264	3.561	3.614	3.438	3.886	3.946	3.566
1 + *Ca*								
Gal^{I}	4.512	3.563	3.548	3.890	3.532	3.783	3.788	
Fuc^{II}	5.114	3.746	3.990	3.830	4.915			1.233
$GlcNAc^{III}$	4.750	4.017	3.894	3.952	3.503	3.917	4.049	2.065
Gal^{IV}	4.443	3.629	3.659	4.145	3.686	3.778	3.817	
Glc^{V}	4.293	3.299	3.604	3.659	3.472	3.898	3.952	3.574
Deviation								
Gal^{I}	0.003	−0.018	0.017	0.020	0.010	**0.042**	**−0.047**	
Fuc^{II}	−0.015	**0.032**	**0.047**	**0.035**	−0.006			−0.017
$GlcNAc^{III}$	−0.014	0.011	**−0.040**	−0.030	0.004	**−0.035**	0.008	0.009
Gal^{IV}	0.004	**−0.047**	**0.032**	0.013	0.020	0.021	**−0.037**	
Glc^{V}	0.018	0.004	0.012	0.014	0.003	−0.019	−0.025	−0.023

[a] **1** + Ca refers to the pentasaccharide **1** with 11.4 equiv of $CaCl_2$. As reference, the carbon and proton signals of the CH_3 group of methanol have been calibrated to (49.0; 3.310) ppm. The bottom part of the Table displays the relative deviations $\Delta\delta - \Delta\delta_{average}$. When they are greater than the threshold 0.03, the corresponding text is bold.

criterion on the potential energy. The rms deviation for the coordinates of their heavy atoms was 0.94 Å.

In both cases, only one or two nOe violations (over 48 and 49 distance constraints, respectively) were found. These discrepancies concern the distances between the anomeric proton of GlcNAc and protons H-2 and H-4 of Gal^{IV}. This corresponds to the cleavage between the rigid Le^{x} motif and the lactose part of the molecule. Therefore, the co-existence of two conformational families in solution could explain the impossibility of representing the experimental data with a simple one-population model. We cannot however prove this point with the NMR data, as, conversely to the case of methyl β-4-carbalactoside in water [40], no significant variation in the local correlation times along the molecule was found. It has to be mentioned, however, that the off-resonance ROESY experiment performed in specific conditions confirms the presence of a strong relaxation leakage in this part of the molecule (measured on proton GlcNAc H-1 and Gal^{IV} H-4). Indeed, when the effective spin-lock field makes an angle of 54°7′ with the static field, a significant discrepancy between the calculated and expected ratios of cross-relaxation rate over self-relaxation rate Γ was observed [23,41]. The difference between the value of 0.5 expected for a purely dipolar relaxation and the experimental value was more important in the presence of calcium. In this last case, about 50% of the self-relaxation of the anomeric proton of the GlcNAc unit does not arise from dipolar re-

laxation, while for all studied protons other than GlcNAc H-1 and Gal H-4, the ratio Γ was close to 0.5. An attempt to ascribe this discrepancy to fast conformational exchange was not conclusive. The reason for this could be that the exchange rate is higher than about 3 MHz, which falls outside the area spanned by our approach.

Calcium titration.—In aqueous media, neutral carbohydrates and polyols form weak complexes with metal cations ($K = 1$–$10\ M^{-1}$). However, in alcoholic media, the association was usually stronger than in water (up to 100-times higher for some furanosides). The cation also influences the reaction by its charge (stronger association with M(III)) and its size (ideal ionic radius seems to be around 1 Å (Na^+, Ca^{2+}, La^{3+}) [8]. Polyols and sugars then have a particularly good affinity with calcium [9]. These behaviours led us to undertake the study of calcium complexation in methanol and dimethyl sulfoxide.

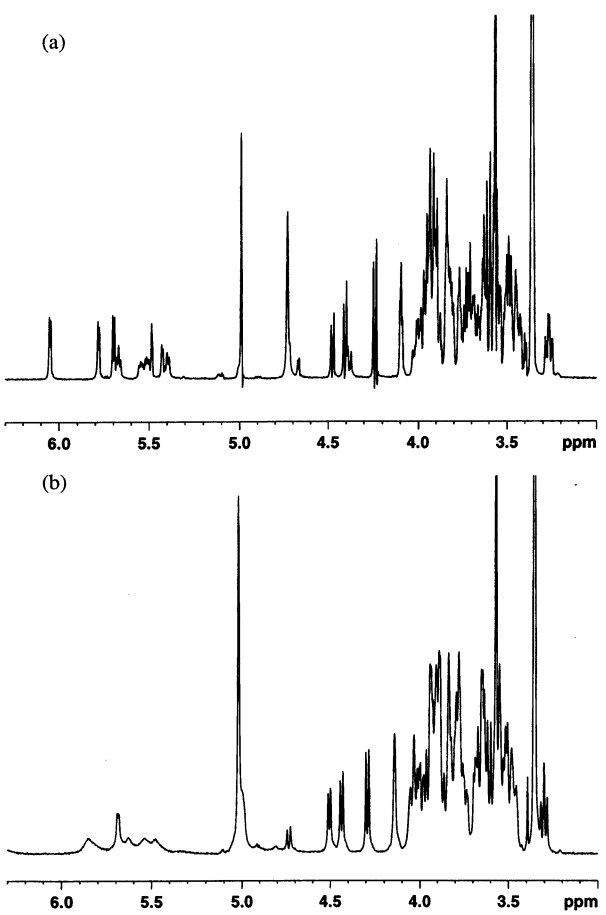

Fig. 1. 500 MHz proton spectrum of **1** at 290 K in CD_3OH (a), and in the presence of 11.4 equiv of $CaCl_2$ (b). Both spectra are obtained with the 3-9-19 WATERGATE pulse scheme [48,49]. The amide proton resonance as well as the methyl signals are voluntarily not plotted.

A simple comparison between the proton spectra of **1** in methanol in the absence and in the presence of calcium (Fig. 1) leads to the following remarks: (i) as expected with the diamagnetic feature of Ca^{2+}, the chemical shift variations are small, but they exist and can be used for determination of the association constant (see below); (ii) no additional lines are observed after addition of the metal, showing that the complexation is fast on the NMR time scale, which is in concordance with literature (the unique case of slow kinetic reported so far is the association of muellitol with lanthanides(III)) [8]; (iii) the exchange rates of the hydroxyl protons with solvent are totally modified, as already noticed by Symons et al. [42,43]. We have checked that it is not due to a pH effect.

To obtain more quantitative values, these exchange rates have been determined using dedicated 1D proton NMR experiments (Fig. 2). In the absence of calcium, the exchange rates of the hydroxyl protons with the solvent were measured around 10 Hz (between 7.6 and 14 Hz). In the presence of calcium, the rates are multiplied by at least a factor 10, except for a particular hydroxyl proton: HO-2 of the Gal^{IV} unit, which passes from 10 to 35 Hz. This proton seems to be involved in a hydrogen bond with the oxygen of the carbonyl group of the GlcNAc unit.

As weak binding constants are expected, care should be taken about the different effects acting on the carbohydrate spectrum during addition of calcium. Beyond the complexation effect, other phenomena such as dilution effect, pH change and variation of macroscopic magnetisation susceptibility can interfere on the chemical shifts. A careful systematic analysis was thus undertaken prior to NMR calcium titration experiments. The dilution effect on the proton chemical shifts was measured independently. This was necessary, as, each calcium chloride molecule being accompanied by two water molecules,

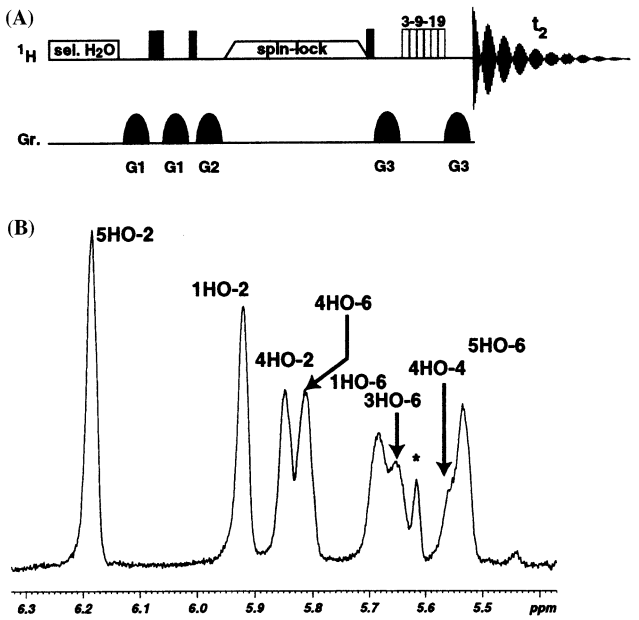

Fig. 2. Measurement of the exchange rates of some hydroxyl protons with methanol. (A) Pulse sequence based on the WEXII filter scheme [50]. Wide and narrow filled boxes represent hard 180 and 90° pulses, respectively. The hydroxyl proton of methanol is selectively excited by a 10 ms Gaussian pulse followed by the WEXII filter. Then, it experiences an off-resonance irradiation with an effective spin-lock field angle of 35°18′, in order to reduce cross-relaxation effects and keep only the exchange peaks [51]. The last step of the sequence is the WATERGATE filter [48,49] designed to suppress the solvent peak. The value of the gradients are: G1 = 3, G2 = 10, and G3 = 7 G cm^{-1}. (B) Example of a 1D subspectrum obtained with 100 ms mixing time.

it could be responsible for a slight chemical shift variation even in dimethyl sulfoxide. Moreover, to minimise it, various concentrations of calcium solutions were used for different parts of the titration curve. Also, care was taken that the minor pH changes occurring upon addition of the calcium solution did not lead to significant chemical shift variations of the proton resonances. The variation of the sample diamagnetic susceptibility led to a global shift of the spectrum, and was consequently taken into account.

Some chemical shift variations as a function of the calcium equivalents used to derive the association constant in dimethyl sulfoxide are shown in Fig. 3. In both solvents, the chemical shifts of some protons vary in the opposite direction from the majority. As an anecdote, a striking effect was observed on the spectrum of **1** in methanol in the presence of 7 equiv of calcium. The doublet of the GlcNAc H-1 signal becomes a triplet, which could lead to the misleading interpretation that another peak appears at the same frequency. The real reason for this effect was that at this cation concentration, the H-2 and H-3 protons resonate at the same frequency, and consequently create very strong coupling conditions, modifying the H-1 and H-4 signals.

The association constant values found for calcium binding are 9.5 M^{-1} in $(CD_3)_2SO$ (using 30 proton resonances), and 29.6 M^{-1} in CD_3OD (using six proton resonances). Assuming an uncertainty of 1.5 Hz on the chemical shift measurement, in the case of methanol, the reduced χ^2 value was 0.54 (59 degrees of freedom). In the case of $(CD_3)_2SO$ it was equal to 4.6 (637 degrees of freedom) and reduces to 2.07 (401 degrees of freedom) when only the experiments with less than 8 equiv of $CaCl_2$ are kept. For these last two fits, the best-fit values of the equilibrium constant K are almost identical. In the case of dimethyl sulfoxide, when a large amount of calcium was added, the discrepancy revealed by the reduced χ^2 shows that either the experimental biases was underestimated or the simple model of complexation between one Ca^{2+} ion and one molecule of **1** was not perfect. This last assumption was corroborated by the results of the study of the paramagnetic ions for which the fits of the experimental data require two locations for the ion (see below).

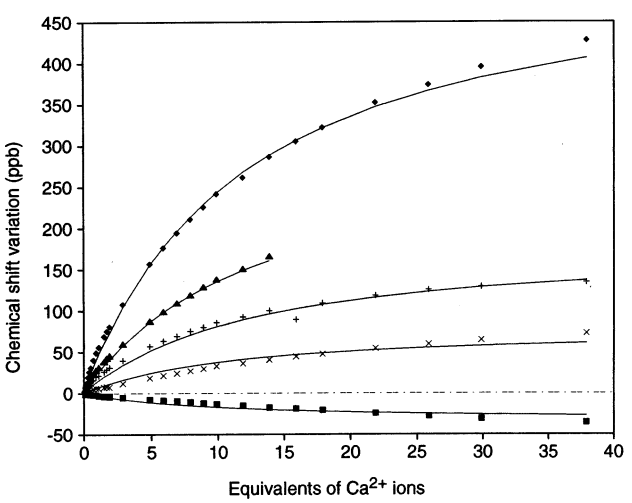

Fig. 3. Chemical shift variation for some protons of **1** in $(CD_3)_2SO$ upon addition of $CaCl_2$. ◆, amide proton of GlcNAc; +, OH-2 of Gal^{IV}; ■, H-6 of Fuc; ×, OH-4 of Fuc; ▲, OH-6 of Gal^{I}.

For such a large excess of calcium, it becomes possible that 1:2 complexes with two calcium ions are formed. The monotonic behaviour of the titration curves (Fig. 3), and the uncertainty on the determination of the experimental error, imply that we are not confident in testing more complicated equilibrium models on the sole basis of the χ^2 value.

The measured binding constants K are greater than those given by Angyal for monosaccharides in water, but lower than the values found for some furanosides in methanol [8]. It is worth noting that oligo- and polysaccharides are known to give stronger complexes than the monosaccharides from which they are issued [10], probably because of the increasing number of binding sites available as well as the capability of cross-linking. In the present case, the low K value indicates that the association constant of a homotypic pentasaccharide–pentasaccharide interaction in the presence of calcium will be too low to be determined by such an approach. Anyway, these results unequivocally prove the presence of a specific interaction between calcium and **1**.

Determination of the interaction sites.—The important point, which can justify the use of NMR spectroscopy as a local descriptor of the molecular events, was the determination of the interaction sites of calcium with the pentasaccharide. In the literature, the complexes formed between sugars or polyols with metal cations are usually tridentate and ascribable to hydroxyl groups (although hydroxymethyl [44], intracyclic [19,45] and interglycosidic oxygen [19] or nitrogen [15] can participate to the reaction). Their formation requires a specific steric arrangement of the electron donor groups, namely *ax*, *eq*, *ax* sequence or 3-*syn*–*ax* (rare in sugars) on six-membered rings, which could help competing efficiently with water molecules for occupancy of the first coordination sphere of a metallic cation. If the reaction is favourable enough, a change in conformation can occur to put the complexing groups in these particular configurations. Nevertheless, the study of structure **1** in the presence of calcium did not reveal the presence of this *ax*, *eq*, *ax* arrangement.

From the proton chemical shifts between the pentasaccharide alone in methanol and in the presence of calcium (Table 2), it could be observed that only some H-2, H-3 and few H-4, H-6 signals experience strong chemical shift variations. According to the chosen threshold, it is remarkable that the H-2, H-3 and H-4 protons of the Gal^I unit did not experience such shifts.

Use of paramagnetic ions.—The use of lanthanide trivalent paramagnetic cations to mimic the influence of the calcium ions was in our hands not so conclusive. Indeed, either the chemical shift variations were too low to be safely interpreted (case of Pr^{3+}, Nd^{3+}, Eu^{3+}, Yb^{3+}, Lu^{3+}), or the relaxation rate variations were quasi-uniform all along the molecule (case of Gd^{3+}). Since, as already noticed, the cation charge is important in such phenomena, we have decided to undertake an NMR study with divalent cations, such as Ni^{2+}, $Co^{2+}$and Mn^{2+}. As detailed below, more significant effects were observed with these ions. Although their ionic radii are slightly smaller than that of Ca^{2+}—respectively 0.69, 0.72 and 0.80 Å—they represented good candidates for mimicking calcium with more important effects on the NMR spectrum.

Divalent manganese, being a symmetrical ion, cannot be used as a chemical shift reagent, as its pseudo-contact contribution vanishes. In contrast, its high electronic spin value (5/2) induces large variations in the relaxation times of the neighbouring nuclei. The expressions of the electronic contribution to nuclear relaxation given by Solomon [46] and Bloembergen [47] indicate that the electronic contribution to self-relaxation time T_1^e is proportional to the distance r_j between the metallic centre and the jth nucleus. It is thus possible (to a first approximation) to write:

$$\frac{1}{T_1^{obs}} = \frac{1}{T_1^{free}} + c\frac{1}{T_1^e} \quad (5)$$

where c is the concentration of paramagnetic spin and $1/T_1^{obs}$ and $1/T_1^{free}$ the longitudinal

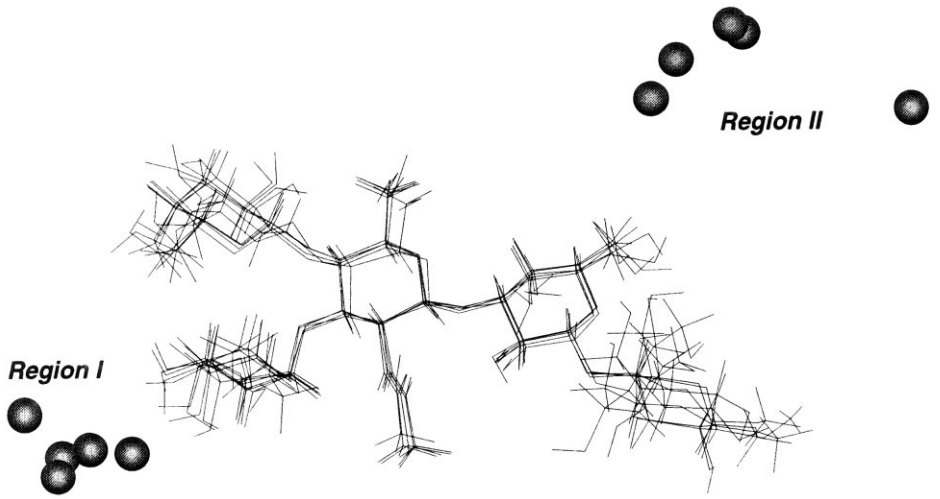

Fig. 4. Superposition of five structures for **1** determined by molecular modelling under NMR constraints with, for each, the average location of the two Mn^{2+} cations. The NMR data have been recorded in the presence of 11.4 equiv of calcium.

self-relaxation rates measured in the presence and in the absence of Mn^{2+}. Moreover:

$$\left[\frac{T_{1i}^{e}}{T_{1j}^{e}}\right]^{1/6} = \frac{r_i}{r_j} \quad (6)$$

Thus, variation of the carbon longitudinal self-relaxation rates of the oligosaccharide was monitored upon addition of $MnCl_2$.

The strong anisotropic magnetic susceptibility of the Co^{2+} or Ni^{2+} ions implies that they constitute good chemical shift reagents. We have undertaken the study on Co^{2+} which presents a larger ionic radius than Ni^{2+}. During cobalt addition, some proton signals were shifted in the opposite direction relatively to what was observed in calcium. This represents an indication that it may be possible to locate the interaction site(s) through triangulation methods. However, the spectral lines were progressively broadened, which shows that this ion also contributes efficiently to transverse relaxation. For this reason, it was impossible to reach the plateau value for which the chemical shifts were no longer affected by the addition of cobalt, and thus to determine the equilibrium constant directly. The beginning of the curve representing, for one proton, the chemical shift variation $\Delta\delta_{obs}$ as a function of the cobalt concentration [Co], confirmed that $\Delta\delta_{obs}$ is linearly proportional to the binding constant K, to [Co], and to the shift in the pure complex $\Delta\delta_{complex}$. In the accessible experimental domain, the ratio of the chemical shift variations of two protons is consequently linearly proportional to the relative variation of $\Delta\delta_{complex}$. This remark was used to relate the relative chemical shift variations with the location of the ion.

Location of Mn^{2+} and Co^{2+} cations.—An attempt to fit the experimental data with the location of a single Mn^{2+} ion was unsuccessful. Indeed large χ^2 values were found, resulting from the incapability of simultaneously minimising the variation of the self-relaxation rates observed on the first hand in the Gal^{I}, Fuc^{II}, $GlcNAc^{III}$ and on the second hand in the Gal^{IV}, Glc^{V} domain. Therefore, a more complex procedure involving two Mn^{2+} ions

Table 3
Main distances defining the location of Mn^{I} and Co^{Ia}

Distance (Å)	Manganese	Cobalt
Distance X–⟨X⟩[b]	0.91	2.85
Distance ⟨Co⟩–⟨Mn⟩[c]	6.6 ± 2.6	6.6 ± 2.6
Distance ⟨X⟩–Gal^{Id}	12.2 ± 0.7	12.0 ± 1.3
Distance ⟨X⟩–Fuc^{d}	9.8 ± 0.7	9.6 ± 1.1
Distance ⟨X⟩–$GlcNAc^{d}$	13.3 ± 0.7	11.0 ± 1.6

[a] The values are computed on the 35 low-energy structures for **1** in the presence of calcium.

[b] Average distance between the minimised ion location and the average one.

[c] Average distance between the average locations of the cobalt ion and of the manganese ion.

[d] Distances between the average paramagnetic ion and the pyranoside unit, computed as the distance between the average ions ⟨X⟩ and the pseudo-atom localised at the barycentre of carbons 1, 3 and 5 of the unit.

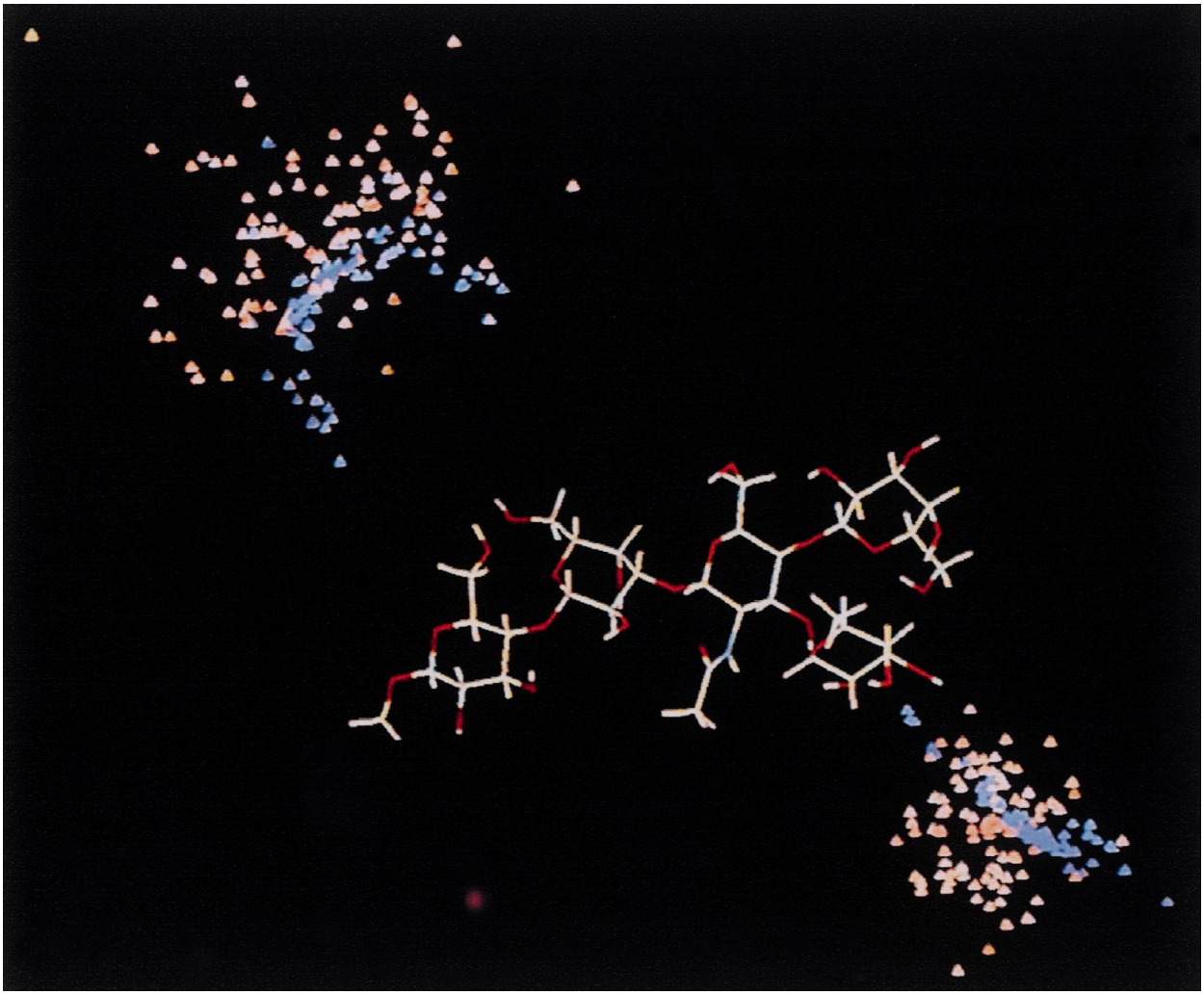

Fig. 5. One low-energy structure for **1** with 2×100 Mn^{2+} ions (blue triangles) and 2×100 Co^{2+} ions (orange triangles) for which coordinates have been determined by the minimisation procedure described in Section 2.

was necessary (see Section 2) as suggested by the fact that polycations are more likely to be found in methanol [6].

Five energy-minimised 3D structures of **1** in methanol with the regions of highest probability for the Mn^{2+} ions are displayed in Fig. 4. Two regions can be discerned: the first one, denoted I, is located at about 10 Å from the nearest atoms of the $Lewis^X$ moiety, equidistant from the Fuc and Gal units. Table 3 summarises the principal statistical results obtained for this location of the manganese ion. The second region, denoted II, is less precise, but is closer to the lactose part. These results, obtained on average locations of the manganese ions, were confirmed when considering a given structure for **1**. In this case, all the accepted locations of Mn^I obtained after the random drawing of initial ionic coordinates, the fit, and the clustering procedure (see Section 2) fall in this region. Fig. 5 shows one of the low-energy structures for **1** with some Mn^{2+} ions resulting from our simulation.

For cobalt, as for manganese, it was necessary to introduce a second cobalt ion in order to fit the data and to explain chemical shift variations for protons in the lactose part as well as in the $Lewis^X$ part of the molecule. The resulting locations of both regions are in good agreement with those found for manganese. The locations found for the cobalt ion are however less precise than the manganese sites even for region I. The average distance between the minimized ion locations and the average one $\langle X \rangle$ increased by a factor of 3 when passing from Mn^{2+} to Co^{2+} (Table 3).

Region II of cobalt is roughly identical to that of manganese. For region I, this lack of precision appears when we compare either the distribution of the cobalt locations for a given structure for **1** (Table 4, Fig. 5), or the average cobalt locations determined for each structure. This is certainly due to the larger number of parameters to fit in the case of the cobalt ion. In our geometry, where the ion is not surrounded by the molecule, a variation of the ion coordinates can be, at least partially, compensated by a variation of the orientation of the principal axis of the paramagnetic susceptibility tensor to give the same effect on the NMR data. Anyway, there is still a site of interaction near the Lewis^X motif, but comparatively to the manganese ion, its distance to the glucosamine unit decreases by about 2 Å (Table 3). It is equidistant from the fucose unit and the methyl group of the glucosamine unit. In fact, the average distances between cobalt and the CO–NH group are about 2.5 Å shorter than for manganese. The broader distribution of the cobalt coordinates in region I leads for some PLEX structures to average distances between cobalt and the CO–NH group of < 6.5 Å, while it is always > 10.0 Å in the case of the manganese. This tends to prove that the difference of locations between cobalt and manganese arises from the influence of the CO–NH group. This difference is certainly due to the smaller size of the Co ion and to different constraints on the symmetry of the complex.

In Table 4, where the distances between the average locations of the paramagnetic ions $\langle X \rangle$ and the heavy atoms of the Lewis^X part are reported, it can be observed that essentially the same atoms of the fucose unit are close to the Co and Mn ions. The effect of the *N*-acetyl group also appears, since distances involving these atoms are found to be short in the cobalt case. Although it does not constitute a formal proof, the protons whose resonances are the most shifted in the presence of calcium, are carried by—or are close to—the heavy atoms of Table 4.

Table 4
Shortest distances between the heavy atoms of the Lewis^X part and the average location $\langle X \rangle$ of the paramagnetic ion[a]

Atom	Manganese		Cobalt	
	Distance (Å)	Rank[b]	Distance (Å)	Rank[b]
Fuc O-3	7.00 ± 0.52	1	8.30 ± 1.90	4
Fuc O-2	7.71 ± 0.59	2	6.71 ± 1.79	1
Fuc C-3	8.27 ± 0.54	3	8.81 ± 1.81	9
Fuc C-2	8.31 ± 0.58	4	7.98 ± 1.84	2
Fuc O-4	8.88 ± 0.49	5		
Gal^I C-6	9.32 ± 0.49	6	9.39 ± 1.82	13
Gal^I O-6	9.37 ± 0.49	7	9.03 ± 1.96	11
Fuc C-1	9.78 ± 0.58	8	8.76 ± 1.76	8
GlcNAc C^{CO}			8.27 ± 1.77	3
GlcNAc C^{CH_3}			8.40 ± 1.92	5
GlcNAc O^{CO}			8.42 ± 1.92	6
GlcNAc N			8.68 ± 1.73	7
GlcNAc O-3			8.87 ± 1.60	10
GlcNAc C-2			9.16 ± 1.78	12
GlcNAc C-3			9.71 ± 1.62	14

[a] Only the distances shorter than 10 Å are reported.
[b] Ranks: distances in increasing order.

4. Conclusion

We have shown, using high-resolution NMR spectroscopy, that a pentasaccharide containing the Lewis^X group interacts with different cations. We have been able to determine the binding constants with calcium in dimethyl sulfoxide and methanol. The value of the binding constant in methanol is not greater than that reported for some furanosides [8]. The expected proportion of 1:100 in the binding constant [22] for complexation of calcium by methyl furanosides in water and in methanol allows us to understand why it is not possible to evidence such an interaction in water for the pentasaccharide through NMR spectroscopy. However, a specific interaction exists, and the solution structures of this pentasaccharide in methanol in the presence and in the absence of calcium have been determined. These molecular structures have allowed the characterisation of the interaction sites between the pentasaccharide and two divalent paramagnetic ions[1] (Co^{2+} and Mn^{2+}). The experimental results indicate that there

[1] The Cartesian coordinates of a low-energy structure for **1** and the associated best-fit locations for the Mn^{2+} and Co^{2+} ions are available upon request from the authors.

is a relatively well-defined region of interaction close to the Lewis^X motif, and a less specified area in the lactose part of the molecule. The results obtained for these two ions are similar but not identical; this is certainly due to the difference of ionic radius and of symmetry of the complexes. The extension to the structure of the calcium complex is obviously not straightforward since these two parameters are different, and the chemical shift variations observed during the formation of the complex result from a diamagnetic effect. However, the similarity of the cobalt and manganese results and the remark that the protons for which chemical shifts are more affected by the addition of calcium (Table 2) are those whose carbons are found to be close to the paramagnetic ions (Table 4), make it reasonable to think that the site of interaction between Ca^{2+} and molecule **1** is located in the vicinity of the fucose unit. These experimental results substantiate Hakomori's hypothesis on the structure of the complex between the Lewis^X and divalent ions, involving homotypic interactions between oligosaccharides.

Acknowledgements

This work was partially funded by a grant from the Centre National de la Recherche Scientifique (CNRS), 'Actions Coordonnées Concertées des Sciences du Vivant (ACC-SV5: Interface Chimie-Physique-Biologie: Biologie structurale et pharmacologie)'.

References

[1] S.I. Hakomori, *Pure Appl. Chem.*, 63 (1991) 473–482.
[2] D.S. Spillmann, M.M. Burger, *J. Cell. Biochem.*, 61 (1996) 562–568.
[3] N.V. Bovin, *Biochemistry* (*Moscow*), 61 (1996) 694–704.
[4] I. Eggens, B. Fenderson, T. Toyokuni, B. Dean, M. Stroud, S.I. Hakomori, *J. Biol. Chem.*, 264 (1989) 9476–9484.
[5] N. Kojima, B.A. Fenderson, M.R. Stroud, R.I. Goldberg, R. Habermann, T. Toyokuni, S.I. Hakomori, *Glycoconjugate J.*, 11 (1994) 238–248.
[6] J.A. Rendleman Jr., *J. Org. Chem.*, 31 (1966) 1839–1845.
[7] S.J. Angyal, *Tetrahedron*, 30 (1974) 1695–1702.
[8] S.J. Angyal, *Adv. Carbohydr. Chem. Biochem.*, 47 (1989) 1–43.
[9] J. Mills, *Biochem. Biophys. Res. Commun.*, 6 (1961) 418–421.
[10] S.J. Angyal, J.A. Mills, *Aust. J. Chem.*, 32 (1979) 1993–2001.
[11] S.J. Angyal, D.C. Craig, *Carbohydr. Res.*, 241 (1993) 1–8.
[12] F. Cadet, *Spectrosc. Lett.*, 29 (1996) 1353–1365.
[13] P. Rongère, N. Morel-Desrosiers, J.-P. Morel, *J. Chem. Soc., Faraday Trans.*, 91 (1995) 2771–2777.
[14] A. Vesala, R. Käppi, *Polyhedron*, 4 (1984) 1047–1050.
[15] M. Miyazaki, S. Nishimura, A. Yoshida, N. Okubo, *Chem. Pharm. Bull.*, 27 (1979) 532–535.
[16] K. Dill, D. Carter, *Adv. Carbohydr. Chem. Biochem.*, 47 (1989) 125–166.
[17] G. Siuzdak, Y. Ichikawa, T.J. Caulfield, B. Munoz, C.-H. Wong, K.C. Nicolaou, *J. Am. Chem. Soc.*, 115 (1993) 2877–2881.
[18] S. Penn, M. Cancilla, C. Lebrilla, *Anal. Chem.*, 68 (1996) 2331–2339.
[19] G. Siuzdak, Z.-L. Zheng, J.Y. Rhampal, Y. Ichikawa, K.C. Nicolaou, F.C.A. Gaeta, K.S. Chatman, C.-H. Wong, *Bioorg. Med. Chem. Lett.*, 4 (1994) 2863–2866.
[20] P. Brocca, P. Berthault, S. Sonnino, *Biophys. J.*, 74 (1998) 309–318.
[21] M.R. Wormald, C.J. Edge, R.A. Dwek, *Biophys. Biochem. Res. Commun.*, 180 (1991) 1214–1221.
[22] H. Lönnberg, A. Vesala, R. Käppi, *Carbohydr. Res.*, 86 (1980) 137–142.
[23] H. Desvaux, P. Berthault, N. Birlirakis, M. Goldman, *C.R. Acad. Sci. Paris, Sér. II*, 317 (1993) 19–25.
[24] H. Desvaux, P. Berthault, N. Birlirakis, *Chem. Phys. Lett.*, 233 (1995) 545–549.
[25] P. Berthault, N. Birlirakis, G. Rubinstenn, P. Sinaÿ, H. Desvaux, *J. Biomol. NMR*, 8 (1996) 23–35.
[26] I. Lundtiand, C. Pedersen, *Acta Chem. Scand., Ser. B*, 30 (1976) 680–684.
[27] R.K. Jain, K.L. Matta, *Carbohydr. Res.*, 226 (1992) 91–100.
[28] H. Lönn, *Carbohydr. Res.*, 139 (1985) 105–113.
[29] G.H. Veeneman, S.H. Van Leeuwen, J.H. Van Boom, *Tetrahedron Lett.*, 31 (1990) 1331–1334.
[30] T. Ehara, A. Kameyama, Y. Yamada, H. Ishida, M. Kiso, A. Hasegawa, *Carbohydr. Res.*, 281 (1996) 237–252.
[31] J. Dahmen, G. Gnosspelius, A.-C. Larsson, T. Lave, G. Noori, K. Palsson, *Carbohydr. Res.*, 138 (1985) 17–28.
[32] L. Müller, *J. Am. Chem. Soc.*, 101 (1979) 4481–4484.
[33] A. Bax, R.H. Griffey, B.L. Hawkins, *J. Magn. Reson.*, 55 (1983) 301–315.
[34] A. Bax, M.F. Summers, *J. Am. Chem. Soc.*, 108 (1986) 2093–2094.
[35] A.T. Brünger, *X-PLOR Version 3.1: a System for X-ray Crystallography and NMR*, Yale University Press, New Haven, 1992.
[36] W.H. Press, W.T. Vetterling, B.P. Flannery, *Numerical Recipes in C. The Art of Scientific Programming*, Cambridge University Press, Cambridge, 1988.
[37] A. Vesala, H. Lönnberg, R. Käppi, J. Arpalahti, *Carbohydr. Res.*, 102 (1982) 312–315.
[38] J. Reuben, *J. Phys.*, 79 (1975) 2154–2157.
[39] L. Banci, I. Bertini, C. Luchinat, *Nuclear and Electron Relaxation*, VCH, Weinheim, 1991.
[40] G. Rubinstenn, P. Sinaÿ, P. Berthault, *J. Phys. Chem. A*, 101 (1997) 2536–2540.
[41] H. Desvaux, P. Berthault, N. Birlirakis, M. Goldman, *J. Chim. Phys.*, 91 (1994) 646652.
[42] M.C.R. Symons, J.A. Benbow, H. Pelmore, *J. Chem. Soc., Faraday Trans. 1*, 78 (1982) 3671–3677.

[43] M.C.R. Symons, J.A. Benbow, H. Pelmore, *J. Chem. Soc., Faraday Trans. 1*, 80 (1984) 2017–2026.
[44] S.J. Angyal, D. Greeves, V.A. Pickles, *Carbohydr. Res.*, 35 (1974) 165–173.
[45] S.J. Angyal, D. Greeves, L. Littlemore, V.A. Pickles, *Aust. J. Chem.*, 29 (1976) 1231–1237.
[46] I. Solomon, *Phys. Rev.*, 99 (1955) 559–565.
[47] N. Bloembergen, *J. Chem. Phys.*, 27 (1957) 572–573.
[48] M. Piotto, V. Saudek, V. Sklenar, *J. Biomol. NMR*, 2 (1992) 661–665.
[49] V. Sklenar, M. Piotto, R. Leppik, V. Saudek, *J. Magn. Reson.*, 102A (1993) 241–245.
[50] S. Mori, J.M. Berg, P.C.M. van Zijl, *J. Biomol. NMR*, 7 (1996) 77–82.
[51] H. Desvaux, P. Berthault, N. Birlirakis, M. Goldman, M. Piotto, *J. Magn. Reson. A*, 113 (1995) 47–52.